

---

---

**WATER RESOURCES AND THE REGIME  
OF WATER BODIES**

---

---

## **Evolution of the Recharge and Discharge of Groundwater in Plain Area of the Hami Basin from 1959 to 2021**

**Guoqiang Qin<sup>a</sup>, Bin Wu<sup>a,\*</sup>, Mingliang Du<sup>a</sup>, and Bo Wang<sup>a</sup>**

<sup>a</sup> *College of Hydraulic and Civil Engineering, Xinjiang Agricultural University, Urumqi, 830052 China*

*\*e-mail: wbinxj@126.com*

Received July 10, 2023; revised October 14, 2023; accepted October 16, 2023

**Abstract**—Groundwater serves crucial roles in resource preservation, ecological maintenance, and geological security in addition to being a significant component of water supplies. This work meticulously summarized data on the growth and consumption of water resources, hydrogeological survey, and groundwater inquiry and evaluation since 1959 to 2021 to estimate the evolution of the recharge, discharge, and storage of groundwater in the Hami Basin. The results suggest that: 1) Human activities primarily influenced the evolution of the groundwater recharge and discharge factor in the Hami Basin, and the abrupt changes in recharge and discharge were consistent with the implementation of policies such as reform and opening up and western development, which is a key factor in controlling human activities; 2) Total groundwater recharge fell from  $8.22 \times 10^8 \text{ m}^3/\text{a}$  in 1959 to  $4.08 \times 10^8 \text{ m}^3/\text{a}$  in 2021. The discharge of groundwater has reduced from  $8.21 \times 10^8$  in 1959 to  $5.67 \times 10^8 \text{ m}^3/\text{a}$  in 2021; and 3) The equilibrium between groundwater recharge and discharge was disrupted in 1975, and ever since then, the discharge has always been greater than the recharge, indicating a negative equilibrium state. The total amount of storage over the last 45 years was  $-71.3 \times 10^8 \text{ m}^3$ .

**Keywords:** Hami Basin, groundwater, recharge and discharge, storage variable, evolution

**DOI:** 10.1134/S0097807823601589

### INTRODUCTION

Groundwater is a significant component of water resources and is crucial for resource security, ecological preservation, and geological security [8]. Especially in arid areas lacking precipitation, groundwater is essential for maintaining environment's health and supplying water. Groundwater resources in certain regions are facing major issues including excessive exploitation and contamination in recent years due to human activity and climate changes [2]. Regional ecological and geological security, as well as water safety are seriously impacted [14, 18]. Understanding the evolution pattern of groundwater resources is important for better managing and protecting them as well as for ensuring the safety of water, ecology, and geology. With the advancement of drilling and mining, and technologies over the past few decades, the extraction operations have substantially risen, which has caused a fall in groundwater level. In many arid regions, excessive exploitation and poor management have resulted in groundwater depletion and deterioration of water quality. A series of consequences such as ecosystem deterioration, surface water runoff reduction and wetland disappearance, and desertification have gradually occurred, all of which are related to the excessive exploitation of groundwater. In addition to these anthropogenic mining activities, the water resources

in arid and semi-arid areas are also threatened by climate change. Climate change and water resources problems have increased the challenge of groundwater sustainability. With the growth of population, the demand for domestic water and agricultural water is increasing, which puts more strain on available water supplies. In consequence, the sustainability of groundwater has become a major concern of many countries. The alteration of groundwater flow field and the evolution of groundwater resources in extremely arid areas must be revealed.

Numerous research on the evolution of groundwater resources system in arid areas have been conducted [9]. For example, Feng et al. [6] studied the main causes and characteristics of the alteration of groundwater flow field in Shijiazhuang area in the past 40–50 years. Shi et al. [15] studied the evolution pattern of groundwater and its depression funnel in North China Plain since the 1950s. Wu et al. [16] performed a quantitative analysis on the relationship between the recharge of groundwater and the discharge of karez wells in Shanshan County in the past 60 years. Van Engelenburg et al. [5] studied the impact of climate change on the exploitation of groundwater in the Netherlands. Le Brocque et al. [1] studied the relationship between the change of groundwater level and irrigation in Southern Queensland, Australia from 1989 to 2015. In summary, previous studies mainly

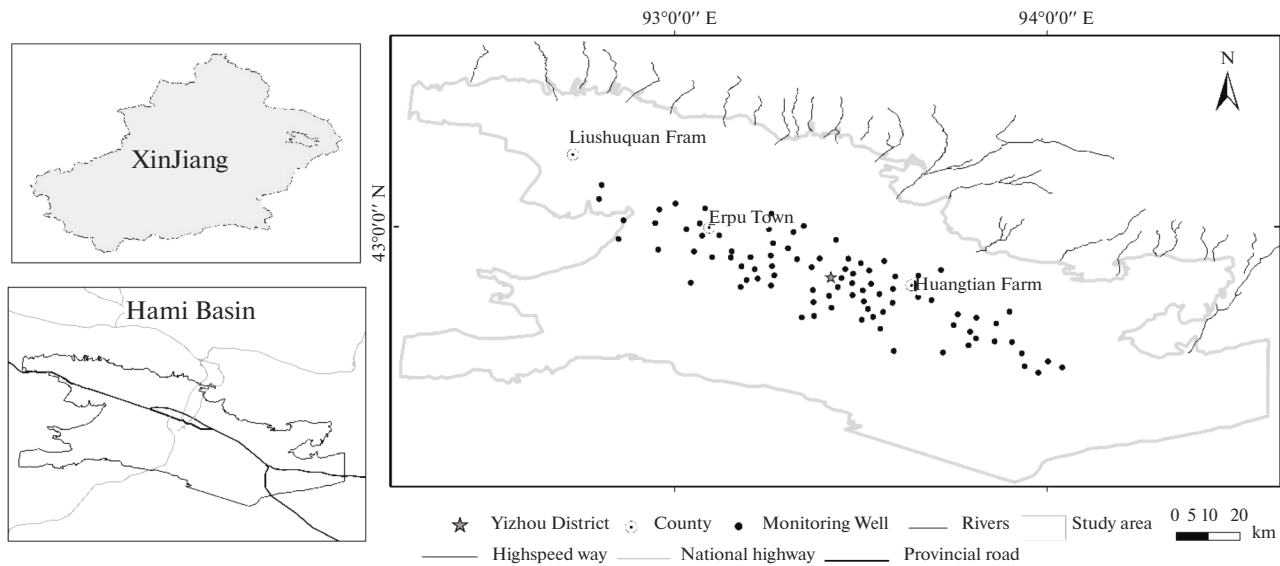


Fig. 1. Topography and water systems in the Hami Basin.

focused on the characteristics of one or more components of the local groundwater system's recharge or discharge. For the rational development and utilization of regional groundwater resources, it is necessary to make a comprehensive assessment of the different recharge, discharge, and water balance of the aquifer system.

The extremely arid Hami basin in Xinjiang is studied in this paper, with an aim to reveal the evolution of the groundwater system. According to the data and other results collected during 1959–2020 [5, 7, 9, 11, 12, 15, 17, 18], the recharge and discharge structures of groundwater resources during 1959–1975, 1975–1990, 1990–1996, 1996–2003, 2003–2011 and 2011–2020 are compared. The evolution process of the recharge and discharge systems as well as storage variables of groundwater resources in the Hami basin in the past 60 years is analyzed. The elements that influence the modification of groundwater supplies are examined. The research findings will contribute to establishing a scientific foundation for the sensible development, usage, and protection of groundwater resources in this region.

## MATERIALS AND METHODS

### *Study Area*

The Hami basin is situated in the east of Xinjiang, China. The administrative division covers the Yizhou District of Hami City and the six regiments of the 14th division of the Corps. The basin is surrounded by mountains in the north, east and south, and separated from the Turpan Basin by hills in the west, which is an almost enclosed basin. In general, the topography is high in the northeast and low in the southwest. The

Shal Lake is the lowest point in the basin (the center of the catchment, which is now dry). The basin has an area of about  $2 \times 10^4$  km<sup>2</sup>, with an altitude of 700 to 1500 m. The basin is wide in the west and narrow in the east, spanning approximately 250 km from east to west, and 100 km from north to south (Fig. 1).

The Hami Basin is distinguished by a typical continental arid desert climate in a mild temperate zone, with high temperatures and little rain, due to its unique geographic location and topography. The annual average temperature is 10°C. The annual average precipitation is 39.4 mm, while the yearly evaporation is 2780 mm. The water systems in the Hami basin are originated from the middle and high mountains in the north, and their supply comes from the melting water of ice and snow and precipitation in mountainous areas. The direction of runoff is from the mountainous area to the plain area, and finally enters the Shal Lake in the center of the basin. There are 28 rivers in the basin, with an average annual runoff of  $3.64 \times 10^8$  m<sup>3</sup>. Among them, there are 16 rivers belonging to the Balikunshan water system, with a total average annual runoff of  $1.25 \times 10^8$  m<sup>3</sup>. There are 12 rivers belonging to the Ka'erlikeshan water system, with a total average annual runoff of  $2.39 \times 10^8$  m<sup>3</sup>.

The aquifer in the plain area of the Hami Basin mainly consists of gravel and sand. From north to south, the particles of aquifer change from coarse to fine, and the burial depth of groundwater changes from deep to shallow [14]. The groundwater near the piedmont is dominated by phreatic water, and the confined water is mainly distributed in the center. The runoff direction of the groundwater is generally consistent with the topographic gradient, which is from the northeast to the southwest, and finally flows into

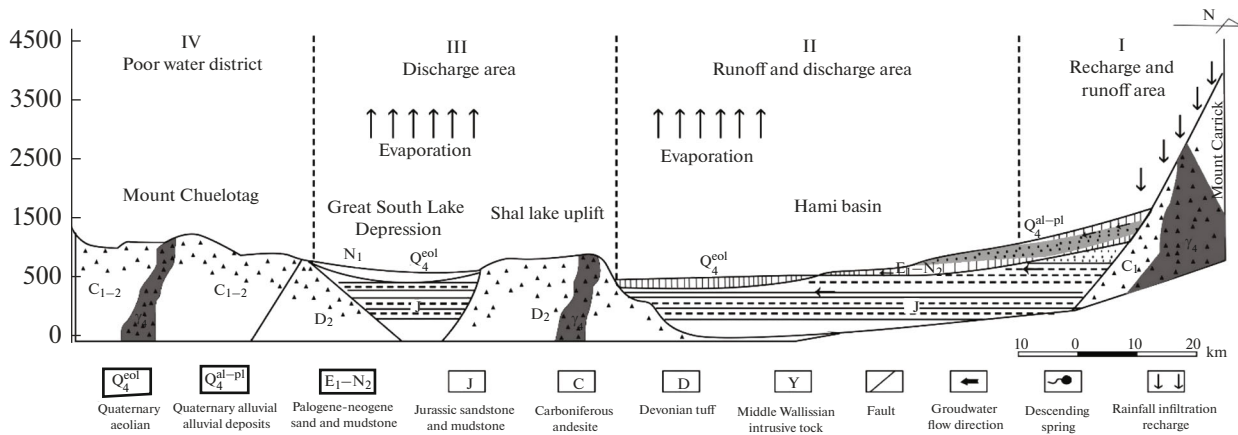


Fig. 2. A simplified hydrogeological diagram of the A–A' section of the Hami Basin.

the Shal Lake. The annual variation of groundwater level in the basin is obviously affected by artificial exploitation. In the past 45 years, the overall groundwater level has been continuously decreasing, with a cumulative decrease of approximately 60 m in some areas (Fig. 2).

Data Collection

Through combing all the historical data of water resources utilization in the Hami Basin in the past 60 years, it has been discovered that the pertinent data on groundwater primarily originate from six periods. The groundwater recharge (lateral infiltration recharge, river valley undercurrent, river channel infiltration, canal system leakage, reservoir dam leakage and field leakage) and groundwater discharge (evaporation and transpiration discharge, driven well exploitation, karez outflow and spring overflow) data are from “the comprehensive evaluation report of environmental geology in the Hami Basin” in 1959, “the planning report of groundwater resources development and utilization in Hami City” in 1997, “the description of 1 : 200000 hydrogeological map of Hami County” in 1980, “the evaluation of groundwater resources in Hami Area” in 2006, “the exploration report on groundwater in coal base and the Hami Basin in eastern Xinjiang” in 2011, and “the study on the evolution law of groundwater system in the Hami Basin from 1960 to 2020” in 2021. The above data are from field investigation and real-time observation. To explore the evolution pattern of the groundwater recharge and drainage system in the Hami Basin under the interference of human activities, the analysis of the evolution of the groundwater system used 1959 as the reference period, and 1990, 1996, 2003, 2011 and 2021 as the comparative periods.

Water Level Monitoring

Groundwater monitoring in Hami Basin began in 1970, and the method of measuring cup was used. After 1990, a special groundwater monitoring work was established in the basin system, which was measured by electric contact suspended hammer gauge. Since 2012, the basin has adopted the automatic monitoring method that can direct solid state storage and telemetry transmission. At present, 68 monitoring Wells have been built, mainly in the irrigation area of the oasis plain, with a monitoring area of 2469 km<sup>2</sup> and a density of 27 holes/10<sup>3</sup> km<sup>2</sup>.

Calculation Method of Recharge

The recharge is composed of the lateral infiltration recharge, river valley undercurrent, precipitation infiltration (since there is almost no secondary precipitation of more than 10 mm in the plain area of the Hami Basin, the precipitation infiltration can be ignored), and surface water conversion recharge (including river infiltration, canal system seepage, reservoirs and dams seepage, and field seepage).

**Lateral infiltration recharge.** The lateral runoff calculation section is established according to the exploration holes in the Gobi belt in front of the mountain. The lateral recharge ( $Q_{tir}$ ) is obtained by deducting the river channel infiltration ( $Q_{trci}$ ) and the river valley undercurrent ( $Q_{trvu}$ ) from the cross-section runoff ( $Q_{tcr}$ ) (Eq. (1)).

$$Q_{tir} = Q_{tcr} - Q_{trci} - Q_{trvu} \tag{1}$$

In this paper, the section method is adopted to calculate the cross-section runoff (Eq. (2)).

$$Q_{tcr} = KIHL \times 365 \sin \alpha, \tag{2}$$

where  $Q_{tcr}$  is the lateral recharge (10<sup>8</sup> m<sup>3</sup>/a),  $K$  is aquifer hydraulic conductivity (m/d),  $H$  is the average thickness of the aquifer at the calculated cross-section

(m),  $L$  is the length of the calculated cross-section (m),  $I$  is the groundwater hydraulic gradient (%), and  $\alpha$  is the angle between calculated section and the groundwater flow direction ( $^\circ$ ).

The groundwater conversion recharge mainly refers to the volume of water that is infiltrated and replenished into the ground during the use of groundwater from driven wells, karez wells and spring water.

**River valley undercurrent recharge.** The river valley undercurrent refers to the lateral inflow of the underground runoff (undercurrent) from the mountain valley to the piedmont plain. In this study, the section method is utilized to calculate the undercurrent recharge of river valleys with borehole control. According to the runoff supply conditions and geomorphic characteristics, the river valleys without borehole control are divided into various types, scales, and runoff sizes. The river valley undercurrent was calculated by analogy (Eq. (3)).

$$Q_{trvu} = 365KIHL, \quad (3)$$

where  $Q_{trvu}$  is the river valley undercurrent,  $K$  is the aquifer hydraulic conductivity (m/d),  $I$  is the hydraulic gradient (%),  $H$  is the average thickness of the aquifer (m),  $L$  is the width of the cross-section (m).

**River infiltration recharge.** Rivers are significant sources of groundwater recharge in arid and semi-arid regions. For the groundwater recharge and drainage system, an accurate estimate of the river infiltration recharge is crucial [3] (Eq. (4)).

$$Q_{trir} = (Q_{tarv} - Q_{tacd})\beta, \quad (4)$$

where  $Q_{trir}$  is the river infiltration recharge ( $10^8 \text{ m}^3/\text{a}$ ),  $Q_{tarv}$  is the annual runoff volume of the river ( $10^8 \text{ m}^3/\text{a}$ ),  $Q_{tacd}$  is the annual channel diversion ( $10^8 \text{ m}^3/\text{a}$ ), and  $\beta$  is the river infiltration recharge coefficient.

**Canal system seepage recharge.** The canal system seepage recharge refers to the seepage recharge of groundwater by all levels of channels before surface water enters the field through diversion irrigation channels [13] (Eq. (5)).

$$Q_{taocssr} = Q_{taowd}(1 - \eta)\gamma\gamma', \quad (5)$$

where  $Q_{taocssr}$  is the amount of canal system seepage recharge ( $10^8 \text{ m}^3/\text{a}$ ),  $Q_{taowd}$  is the amount of water diverted at the head of the canal ( $10^8 \text{ m}^3/\text{a}$ ),  $\eta$  is the comprehensive utilization coefficient of the canal system,  $\gamma$  is the correction coefficient of the canal leakage,  $\gamma'$  is the correction coefficient of the canal system impermeability.

**Field seepage recharge.** The field seepage recharge refers to the volume of groundwater replenished by the vadose zone after the canal water (surface water) enters the field [10] (Eq. (6)).

$$Q_{tfl} = Q_{c-f}\beta_{tflc}\gamma, \quad (6)$$

where  $Q_{tfl}$  is the field leakage ( $10^8 \text{ m}^3/\text{a}$ ),  $Q_{c-f}$  is the amount of surface water introduced by channels into the irrigated area of the field,  $\beta_{tflc}$  is the field leakage coefficient ( $10^8 \text{ m}^3/\text{a}$ ), and  $\gamma$  is the correction coefficient.

**Reservoirs and dams seepage recharge.** The seepage recharge of the reservoirs and dams could be calculated using (Eq. (7)).

$$Q_{tri} = Q_k a_{tric}, \quad (7)$$

where,  $Q_{tri}$  is the reservoir leakage ( $10^8 \text{ m}^3/\text{a}$ ),  $Q_k$  is the average reservoir capacity over the years or perennial storage volume ( $10^8 \text{ m}^3/\text{a}$ ), and  $a_{tric}$  is the reservoir leakage coefficient.

### Calculation Method of Discharge

The available discharge of groundwater includes the exploitation of driven wells, the discharge of karez wells, and the overflow of spring water. The exploitation of driven wells can be obtained by the distributed water meter reader, which realizes the wireless data acquisition through the infrared communication port. The data is input into the computer in the form of text and is finally processed by the specialized software. The discharge of karez wells and the overflow volume of spring water are determined by field investigation and manual measurement.

Indirect groundwater discharge denotes groundwater evapotranspiration discharge, where groundwater evapotranspiration discharge in irrigated and irrigated areas are calculated separately. The evapotranspiration discharge of groundwater from irrigated areas was calculated using (Eq. (8)).

$$E_{cg} = 10^{-5} E_{601} C F \left( C' \frac{E_{601.1}}{E_{601}} - \frac{E_{601.1}}{E_{601}} \right), \quad (8)$$

where  $E_{cg}$  is the groundwater evaporation and transpiration in irrigated areas ( $10^8 \text{ m}^3/\text{a}$ ),  $E_{601}$  is the annual water surface evaporation (mm),  $C$  is the groundwater evaporation coefficient,  $F$  is the area of the calculation region ( $\text{m}^2$ ),  $C'$  is a correction coefficient of depending on the evaporation from vegetation under crop cover conditions (the cover rate is taken as 90%),  $E_{601.1}$  is the water surface evaporation during crop growth and maturation (April–September) (mm).

### Calculation Method of Variation of Groundwater Storage

The variation of groundwater storage was calculated using (Eq. (9)).

$$\Delta w = 10^{-2} (Z_1 - Z_2) \mu F, \quad (9)$$

where  $\Delta w$  is the change in groundwater storage volume during the calculation period ( $10^8 \text{ m}^3$ ),  $Z_1$  is the average groundwater table depth at the beginning of the calculation period (m), and the area-weighted method is used to determine the initial monitoring value based

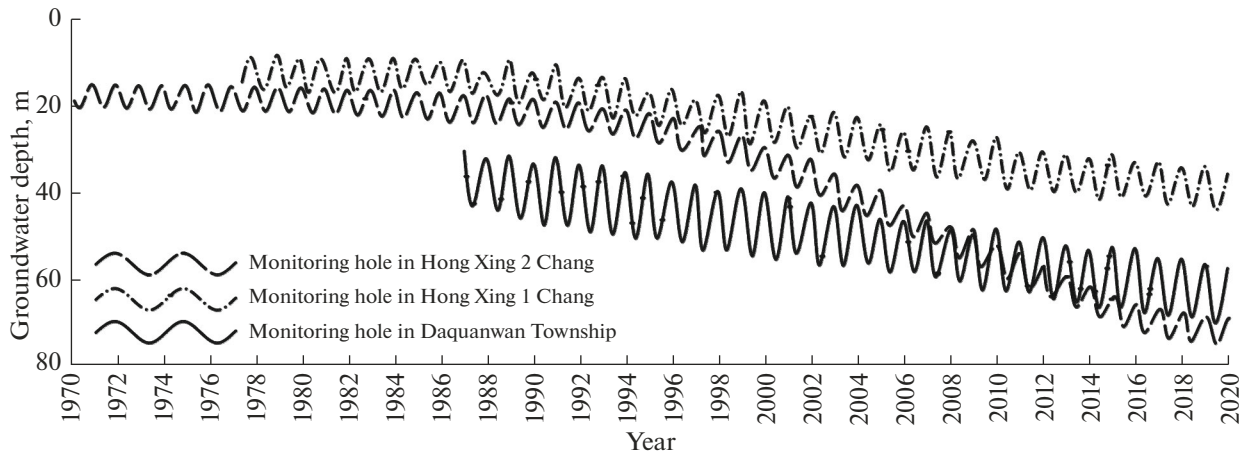


Fig. 3. Evolution curve of groundwater level in typical groundwater monitoring holes in Hami Basin.

on the data of each groundwater table depth in the monitoring well,  $Z_2$  is the average groundwater table depth at the end of the calculation period (m), and the area-weighted method is used to determine the end monitoring value based on the data of each groundwater table depth in the monitoring well,  $\mu$  is the specific yield of the geotechnical layer between  $Z_1$  and  $Z_2$  dimensionless, using the results of previous results in this area in recent years, see Fig. 3, and  $F$  is the area ( $\text{km}^2$ ).

## RESULTS AND DISCUSSION

### *Temporal and Spatial Evolution of Groundwater Flow Field*

According to historical monitoring data, the groundwater level in the Hami Basin has been continuously declining since 1975 (Fig. 3). The monitoring data can be divided into three stages.

(1) From 1975 to 1990, the decline rate of some areas gradually increased. Erpu Town and Huangtian Farm were the major sites where the groundwater level fell during this time. Because these areas were the first to open up wasteland and drill wells, the discharge was greater than the recharge. The groundwater level began to decline throughout the entire basin, with a decline range of 0.1 to 0.9 m/a. The decline areas continued to expand, and the annual decline rate gradually increased.

(2) Rapid decline stage from 1990 to 2016: the decline rate of groundwater level in the oasis plain area of the whole basin showed an accelerated trend. The decline areas extended from part of Erpu Town and Huangtian Farm to the whole oasis plain and its surrounding areas. Four depression funnels were formed from west to east, namely, the Erpu-Sancun funnel, West Gobi funnel, Yawulong Development Zone funnel, and Daquanwan-Huanglonggang funnel. The oasis plain area of the whole basin declined at an aver-

age rate of 0.86 m/a. Hongxing Erchang displayed the largest decline rate of 2.09 m/a. The local cumulative decline reached 51 m.

(3) From 2016 to 2020, the decline rate gradually decreased. Excessive exploitation of groundwater has been controlled in the basin. Water levels dropped while the land withdrew. The driven wells had been covered or shut. There was less groundwater exploitation overall. The continuous declining trend of groundwater level near the piedmont in the periphery of the oasis plain area was alleviated, but the groundwater level in the center of the irrigation area with high mining intensity of mechanical wells still declined rapidly. In the entire basin, the groundwater level decreased at an average rate of 0.32 m/a in the oasis plain region. The West Gobi's overexploited area has the quickest declining rate, with an average drop rate of 0.59 m/a (Fig. 4).

### *Evolution of Groundwater Recharge and its Influencing Factors*

The evaluation results of groundwater recharge in the plain area of the Hami Basin from 1959 to 2020 are displayed in Table 1. The total groundwater recharge in 1959, 1975, 1990, 1996, 2003, 2011, 2016 and 2020 was  $8.22 \times 10^8$ ,  $8.26 \times 10^8$ ,  $7.65 \times 10^8$ ,  $7.04 \times 10^8$ ,  $5.82 \times 10^8$ ,  $5.09 \times 10^8$ ,  $4.6 \times 10^8$ , and  $4.08 \times 10^8 \text{ m}^3$ , respectively. The change of recharge can be divided into three stages:

1. Before 1975, the groundwater recharge remained basically stable.

2. From 1975 to 1990, the groundwater recharge declined slowly. The groundwater recharge in 1990 was  $0.61 \times 10^8 \text{ m}^3$  less than that in 1975, with a decrease of 7.4% and an average annual decrease of  $0.04 \times 10^8 \text{ m}^3$ .

3. From 1990 to 2020, the groundwater recharge declined rapidly. The groundwater recharge in 2020

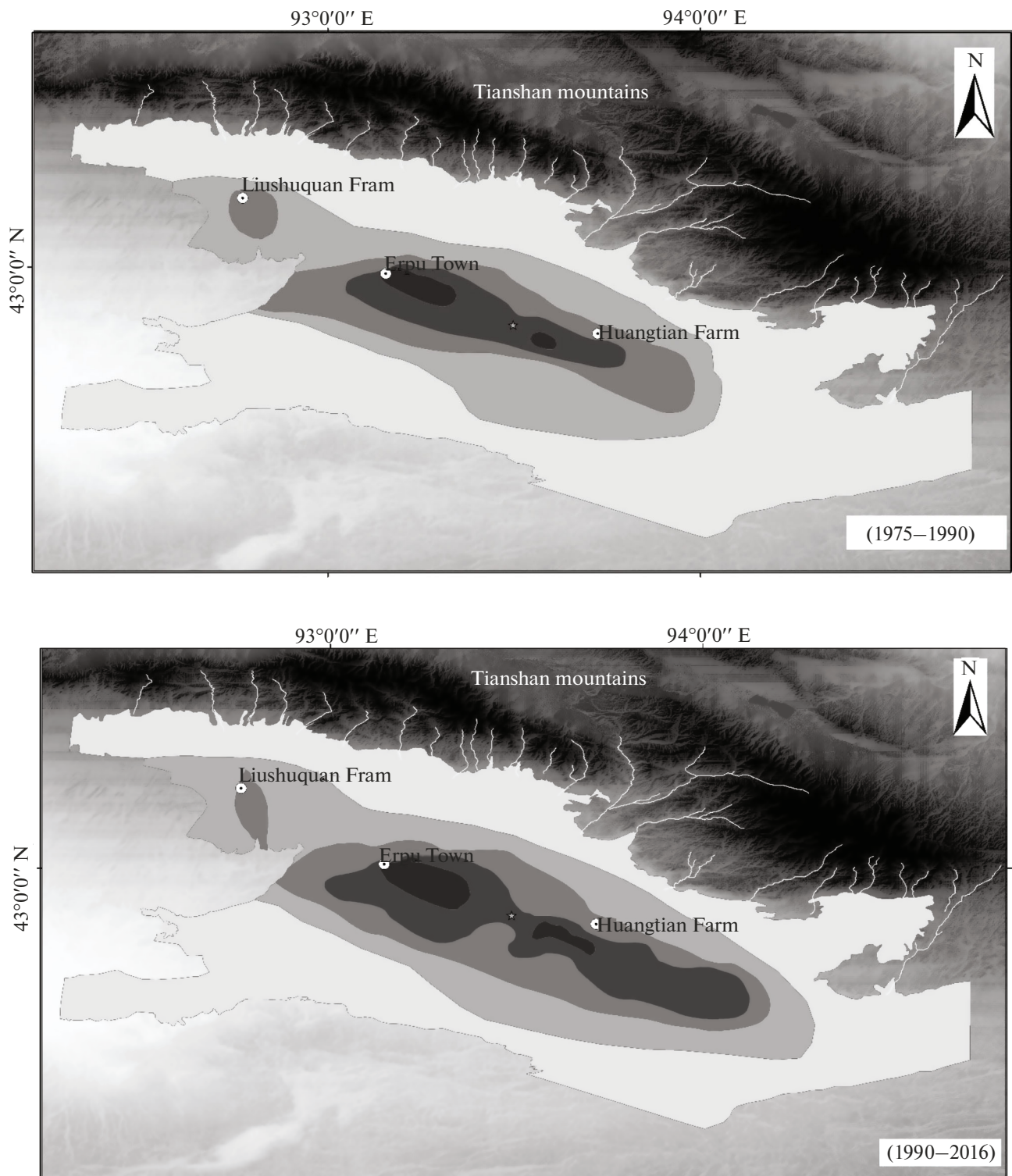


**Fig. 4.** Zoning map of cumulative decline of groundwater in the plain area of the Hami Basin in recent 60 years.

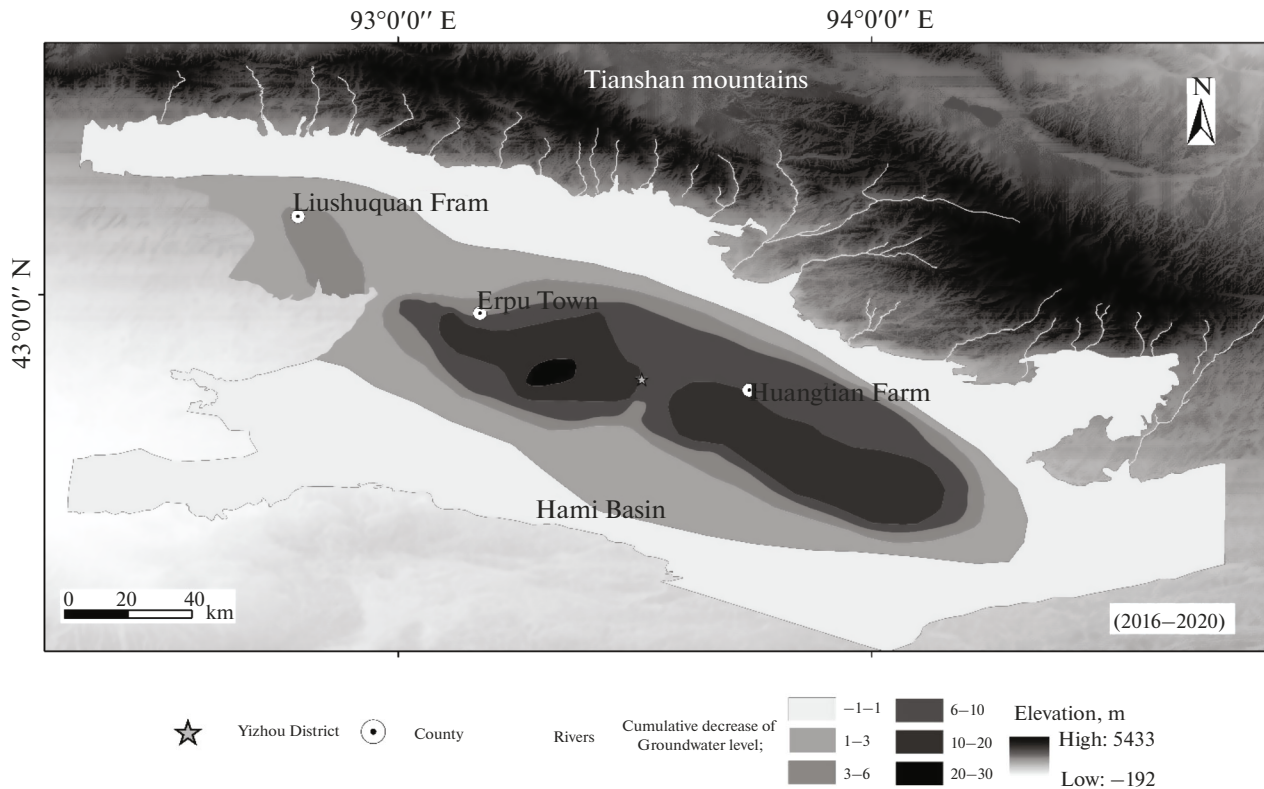


Fig. 4. (Contd.)

was  $3.57 \times 10^8 \text{ m}^3$  less than that in 1990, with a decrease of 46.63% and an average annual decrease of  $0.12 \times 10^8 \text{ m}^3$ .

The Hami Basin's groundwater recharge mode, process, and intensity have seen significant changes over the last 60 years. The conversion recharge of surface water and groundwater was largely steady at first before gradually falling as the natural recharge continued to decline.

In the natural recharge, the lateral infiltration recharge in the piedmont remained stable at about  $1.67 \times 10^8 \text{ m}^3/\text{a}$ . In natural state, the river valley undercurrent is  $0.39 \times 10^8 \text{ m}^3$ . Before 1995, the reservoir building capacity was weak. Afterwards, with the construction of 6 mountain reservoirs such as Yushugou and Miaoergou and 10 canal heads, the river valley undercurrent was almost cut off. Only a few small rivers without blocking projects still have potential flow. The change of the river valley undercurrent can be divided into two stages:

(1) from 1959 to 1996, the potential flow remained basically stable;

(2) from 1996 to 2020, the potential flow declined from  $0.35 \times 10^8$  to  $0.17 \times 10^8 \text{ m}^3$ .

In the surface water conversion recharge, the river channel infiltration is affected by both the runoff of each river and the diversion volume of the channel. In

the past 60 years, the runoff of various rivers in the basin has been basically stable. However, after the 1990s, control reservoirs or river blocking headworks were successively constructed, controlling the surface water and changing the river runoff process and runoff volume. The water diversion volume of the supporting channels increased. The discharge of river decreased. The variation of the river channel infiltration volume was consistent with that of the river valley undercurrent:

(1) from 1959 to 1990, the river channel infiltration volume decreased slowly from  $1.65 \times 10^8$  to  $1.55 \times 10^8 \text{ m}^3$ ;

(2) from 1990 to 2020, the river channel infiltration volume decreased rapidly from  $1.55 \times 10^8$  to  $1.07 \times 10^8 \text{ m}^3$ .

The change of channel leakage was mainly associated with the water diversion volume and the seepage prevention of the channel. Since the 1960s, the main and branch water diversion channels started to be constructed, and the water diversion volume started to increase. Since the 1980s, the channels were built, and the lining rate was increased. The change of channel leakage can be divided into two stages:

(1) from 1959 to 1990, the channel leakage increased slowly from  $1.19 \times 10^8$  to  $1.48 \times 10^8 \text{ m}^3$ ;

**Table 1.** The recharge and dynamic change of groundwater in the plain area of the Hami Basin,  $10^8 \text{ m}^3/\text{a}$ 

Groundwater recharge and discharge items			Groundwater recharge and discharge in different evaluation periods							
			1959	1975	1990	1996	2003	2011	2016	2020
Recharge	Natural recharge items	Lateral leakage in the front of the mountain	1.66	1.67	1.66	1.67	1.65	1.69	1.68	1.66
		River valley undercurrents	0.39	0.38	0.36	0.35	0.27	0.22	0.20	0.17
	Surface water leakage items	River leakage	1.65	1.62	1.55	1.48	1.36	1.24	1.16	1.07
		Channel leakage	1.19	1.24	1.38	1.33	0.95	0.67	0.58	0.50
		Field leakage	0.58	0.57	0.59	0.55	0.36	0.28	0.23	0.18
		Reservoirs leakage	0.08	0.08	0.08	0.08	0.07	0.06	0.06	0.05
	Groundwater conversion recharge items		2.67	2.70	2.03	1.58	1.16	0.93	0.69	0.46
Total recharge		8.22	8.26	7.65	7.04	5.82	5.09	4.60	4.08	
Discharge	Unavailable discharge items	Evapotranspiration	3.42	3.33	3.13	2.85	2.45	1.93	1.25	1.14
		Available discharge items	Overflow of karez wells	2.65	1.86	1.58	1.11	0.87	0.48	0.28
	Exploitation volume of wells		0.00	1.29	2.36	3.63	4.23	5.36	6.21	4.21
	Spring		2.14	1.78	1.27	0.73	0.56	0.25	0.14	0.11
Total discharge		8.21	8.26	8.34	8.32	8.11	8.02	7.88	5.67	

(2) from 1990 to 2020, the channel leakage decreased rapidly from  $1.48 \times 10^8$  to  $0.5 \times 10^8 \text{ m}^3$ .

The change of field infiltration was mainly associated with the volume of water diverted from the field, the irrigation methods in the field and the groundwater level in the irrigation area. Before 1990, the volume of water diverted from the field increased continuously, and then it was basically stable. Before 1980, flood irrigation was the main way in the basin. By 2000, the conventional water-saving irrigation methods such as furrow irrigation and trickle irrigation were promoted. After 2005, the advanced high-tech water-saving irrigation technologies such as drip irrigation were introduced and promoted. The groundwater level in the irrigation area in the basin remained basically stable before 1975, and then continued to decline. In the past 60 years, the field irrigation infiltration in the basin remained at about  $0.55 \times 10^8 \text{ m}^3$  before 1996, and then decreased rapidly from  $0.55 \times 10^8$  to  $0.28 \times 10^8 \text{ m}^3$  from 1997 to 2011. The reduction rate slowed down from 2011 to 2020, and the field infiltration volume in 2020 was  $0.18 \times 10^8 \text{ m}^3$ .

The seepage recharge of reservoirs and dams are mainly comprised of the seepage of plain reservoirs, ponds and Karez waterlogging dams. Before 2011, with

the increase of water diversion, several plain reservoirs were built in the basin, and the infiltration volume increased. After 2011, with the completion of numerous water storage projects, the leakage volume gradually decreased. The seepage recharge of reservoirs and dams first increased from  $0.08 \times 10^8 \text{ m}^3$  in 1959 to  $0.14 \times 10^8 \text{ m}^3$  in 2011, and then decreased to  $0.05 \times 10^8 \text{ m}^3$  in 2021 (Fig. 5).

The groundwater conversion recharge mainly refers to the volume of water that is infiltrated and replenished into the ground during the use of groundwater from driven wells, Karez wells and spring water. This part of infiltration recharge is influenced by multiple factors, including groundwater discharge, the utilization rate of canal and field water, and the groundwater level. The groundwater conversion recharge was  $2.67 \times 10^8 \text{ m}^3$  in 1959 and maintained at about  $2.7 \times 10^8 \text{ m}^3$  until 1975. It declined rapidly to  $0.36 \times 10^8 \text{ m}^3$  during 1996 to 2003, and then declined slowly to  $0.18 \times 10^8 \text{ m}^3$  during 2003 to 2020. It was mainly attributed to the rapid decrease of groundwater discharge, the gradual increase of water utilization coefficient of canal and field, and the gradual decrease of groundwater level.



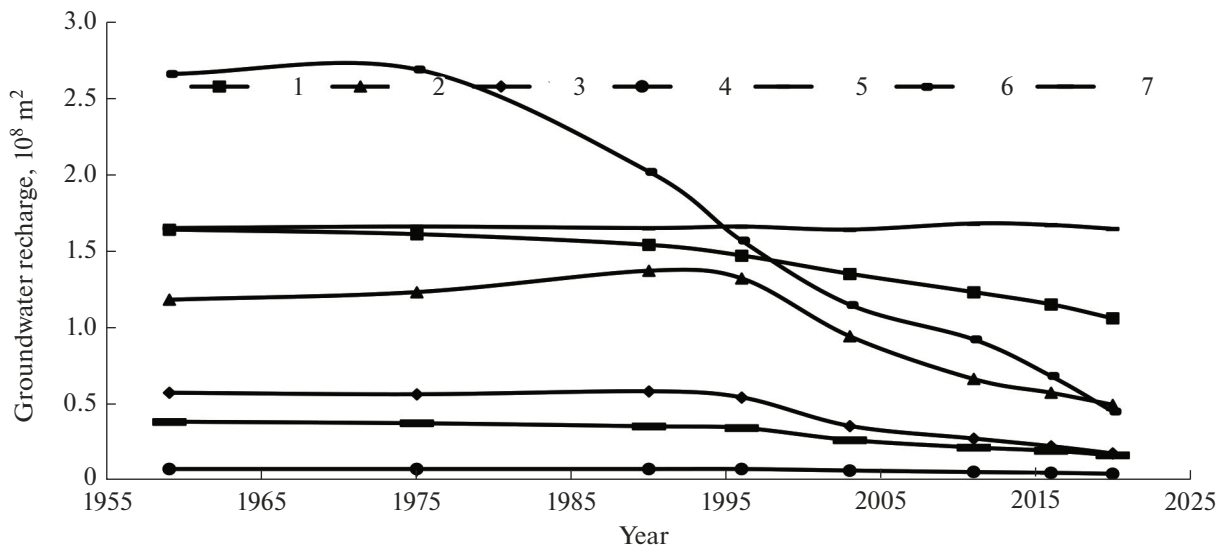


Fig. 5. The curve of groundwater recharge in the Hami Basin in recent 60 years.

#### *Evolution of Groundwater Discharge and its Influencing Factors*

The discharge of groundwater in the plain area of the Hami Basin are comprised of the available and unavailable discharges. The available discharge of groundwater includes the exploitation volume of driven wells and the overflow of karez wells and spring water. The unavailable discharge of groundwater mainly refers to the evapotranspiration discharge.

The evaluation results of the discharge of groundwater in the plain area of the Hami Basin from 1959 to 2020 are present in Table 1. The total discharge of groundwater in 1959, 1975, 1990, 1996, 2003, 2011, 2016 and 2020 was  $8.21 \times 10^8$ ,  $8.26 \times 10^8$ ,  $8.34 \times 10^8$ ,  $8.32 \times 10^8$ ,  $8.11 \times 10^8$ ,  $8.02 \times 10^8$ ,  $7.88 \times 10^8$  and  $5.67 \times 10^8$   $m^3$ , respectively. It remained stable at  $8.3 \times 10^8$   $m^3$  from 1959 to 1996, and declined slowly from  $8.3 \times 10^8$  to  $7.9 \times 10^8$   $m^3$  from 1996 to 2016. Then it declined rapidly from  $7.9 \times 10^8$  to  $5.67 \times 10^8$   $m^3$  from 2016 to 2020, with an average annual decline of  $0.45 \times 10^8$   $m^3$ .

Significant changes in the discharge mode, process, and intensity of groundwater in the Hami Basin have occurred over the last 60 years. The unavailable discharge decreased further, while the available discharge climbed briefly before decreasing further.

The evapotranspiration discharge is the unavailable discharge of groundwater, which is mostly related to groundwater level and vegetation coverage. The evapotranspiration discharge of groundwater in the basin for the last 60 years was computed based on groundwater levels at various times. The evapotranspiration volume remained basically stable at  $3.4 \times 10^8$   $m^3$  from 1959 to 1975, and declined slowly from 1975 to 1990. Then it declined rapidly from  $3.13 \times 10^8$  to

$1.25 \times 10^8$   $m^3$  from 1990 to 2016, which was attributed to the continuous and rapid shrinkage of the area with the buried depth of groundwater  $\leq 6$  m. Afterwards, it declined slowly after 2016. The evolution process was consistent with the continuous decline of the groundwater level in the past 45 years.

In the past 60 years, the variation of available discharge of groundwater in the Hami Basin showed three stages: firstly, increased slowly, then increased rapidly, and finally declined rapidly (Fig. 6). The first stage was from 1959 to 2011, the available discharge increased slowly from  $4.79 \times 10^8$  to  $6.09 \times 10^8$   $m^3/a$ . The second stage was from 2011 to 2016, the available discharge increased rapidly to  $6.63 \times 10^8$   $m^3/a$ . The third stage was from 2016 to 2020, it declined rapidly to  $4.53 \times 10^8$   $m^3/a$ , which was mainly related to the implementation of the "Three Red Lines" policy and the groundwater control policies of Hami City, as well as the reduction of the groundwater exploited by driven wells.

In the past 60 years, the overflow of spring water in the Hami Basin gradually declined from  $2.14 \times 10^8$  to  $0.11 \times 10^8$   $m^3/a$ , which was mainly attributed to the decline of groundwater level.

The variation of the number and discharge of karez wells can be divided into two stages:

(1) from 1959 to 1996, the number of karez wells decreased rapidly with a rate of 6.7/a, and the discharge decreased with a rate of  $0.042 \times 10^8$   $m^3/a$ ;

(2) from 1996 to 2020, the number of karez wells decreased slowly with a rate of 4.4/a, and the discharge decreased with a rate of  $0.038 \times 10^8$   $m^3/a$ ; the decrease of the number and discharge of karez wells was mainly because that the groundwater level dropped below the catchment range of horizontal and

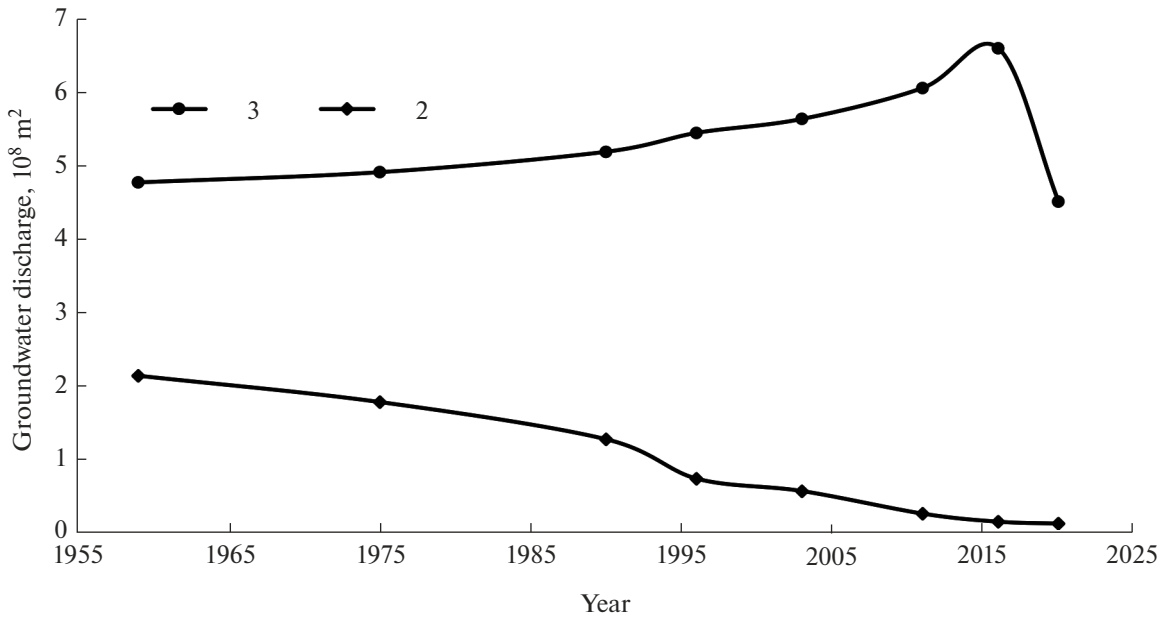


Fig. 6. Evolution curve of the groundwater discharge in the Hami Basin in recent 60 years.

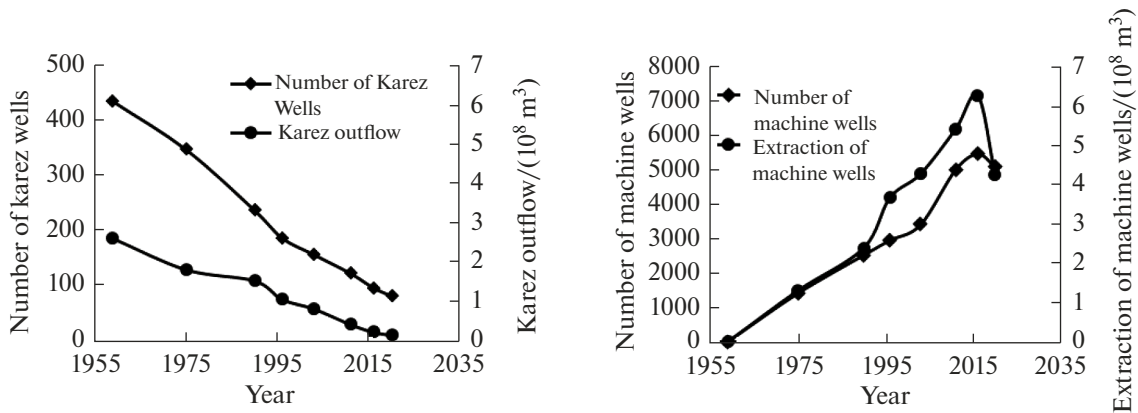


Fig. 7. Evolution curve of the number of karez wells, driven wells and the exploitation volume of groundwater in the Hami Basin.

vertical wells, and the karez wells were lack of maintenance, leading to the collapse of vertical wells and burial of horizontal wells (Fig. 7).

According to available information, the supporting driven wells in the Hami Basin were first used in 1960. After 60 years of development, the exploitation of groundwater by driven wells can be divided into three stages:

(1) From 1960 to 2003, the number of driven wells and the exploitation volume of groundwater slowly increased. In 1960, there were 17 driven wells in the basin, and the annual exploitation volume of groundwater was  $0.01 \times 10^8 \text{ m}^3/\text{a}$ . By 2003, there were 3383 driven wells, with an annual exploitation volume of  $4.23 \times 10^8 \text{ m}^3/\text{a}$ . An average of 77 driven wells were

increased every year, and the annual groundwater exploitation increased by  $0.09 \times 10^8 \text{ m}^3/\text{a}$ .

(2) From 2003 to 2016, the policies of “Western Development” and “Xinjiang Black and White Strategy” were successively introduced, resulting in the large-scale development of land and rapidly increase of the number of driven wells. The annual exploitation of groundwater increased by  $6.21 \times 10^8 \text{ m}^3/\text{a}$ .

(3) From 2016 to present, the number of driven wells and the exploitation volume of groundwater gradually decreased. According to this survey, the exploitation volume of groundwater by driven wells was  $4.21 \times 10^8 \text{ m}^3/\text{a}$  in 2021. The main reason for the decrease should be the implementation of the “Three Red Lines” policy of Hami City in 2016, and the introduction of a series of policies about the groundwater

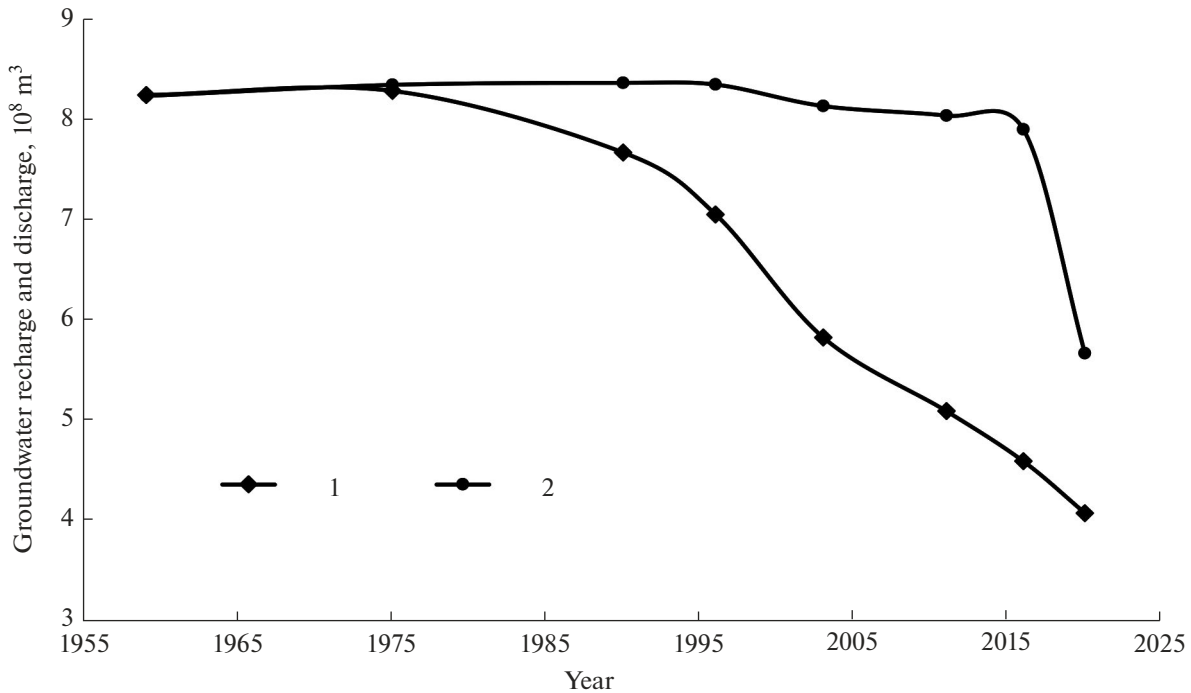


Fig. 8. The evolution of groundwater recharge and discharge in the Hami Basin in the past 60 years.

control, reducing cultivated land, closing driven wells, and limiting the groundwater exploitation of driven wells (Fig. 7).

#### Groundwater Balance Analysis

According to the above analyses of the influencing factors of the groundwater recharge and discharge systems, the evolution process of the recharge and discharge of groundwater in the past 60 years is obtained, as shown in Fig. 8.

As seen by Fig. 8, from 1959 to 1975, the recharge and discharge of groundwater in the Hami Basin remained basically balanced. Since the balance was broken in 1975, the groundwater discharge has been greater than the groundwater recharge, displaying a

negative equilibrium state. From 1975 to 2016, the utilization rate of the static reserves of groundwater increased steadily, with an average annual increase of about  $0.075 \times 10^8 \text{ m}^3/\text{a}$ . The utilization rate of the static reserves was fastest in 2016, reaching  $3.29 \times 10^8 \text{ m}^3/\text{a}$ . Then it declined rapidly to  $1.59 \times 10^8 \text{ m}^3/\text{a}$  in 2020. This is consistent with the governance of groundwater excessive exploitation areas after 2016. According to calculation, the accumulated static reserves of groundwater in the Hami Basin in the past 45 years were  $71.3 \times 10^8 \text{ m}^3$  (Table 2).

The calculation results of groundwater storage variables were used utilized for comparative analysis to check the accuracy of the calculation results of the recharge, discharge, and usage of the static groundwa-

Table 2. Calculation of utilization of the groundwater reserves in the Hami Basin in the past 60 years (Unit:  $10^8 \text{ m}^3/\text{a}$ )

Periods	End-of-period recharges	End-of-period discharges	End of period annual used storage	Annual average used storage	Storage used during the period
1959–1975	8.26	8.32	0.06		
1975–1990	7.65	8.34	0.69	0.42	6.30
1990–1996	7.04	8.32	1.29	1.04	6.22
1996–2003	5.82	8.11	2.29	1.86	13.02
2003–2011	5.09	8.02	2.92	2.65	21.18
2011–2016	4.60	7.88	3.29	3.14	15.71
2016–2020	4.08	5.67	1.58	2.22	8.88
Total					71.31

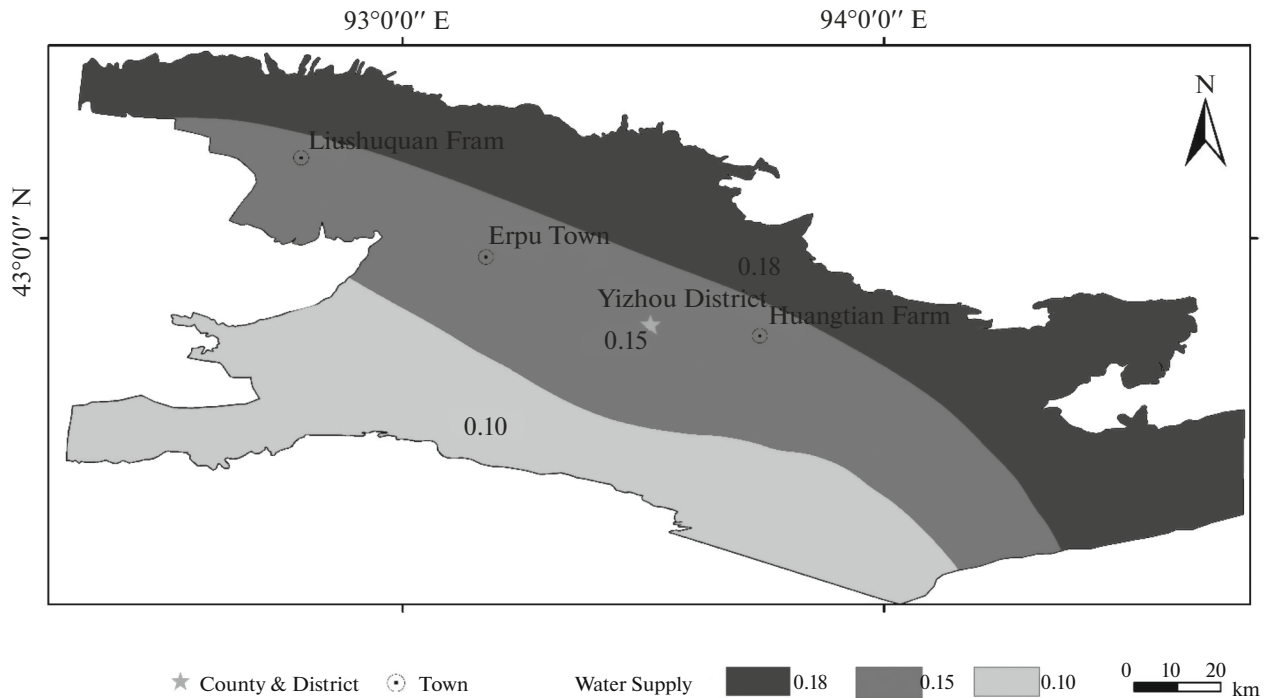


Fig. 9. Water degree zoning map of Hami Basin plain area.

ter reserves. Groundwater supply degree,  $\mu$ , in different regions of Hami Basin is shown in Fig. 9.

According to the calculation, the storage variable was  $-5.58 \times 10^8 \text{ m}^3$  from 1975 to 1990,  $-58.49 \times 10^8 \text{ m}^3$  from 1990 to 2016, and  $-8.23 \times 10^8 \text{ m}^3$  from 2016 to 2020. The accumulated storage variable was  $-72.3 \times 10^8 \text{ m}^3$  from 1975 to 2020.

According to the recharge and discharge balance calculation, the utilized static reserves of the Hami Basin in the past 45 years were  $71.31 \times 10^8 \text{ m}^3$ , which is consistent with the calculation results using this method ( $72.3 \times 10^8 \text{ m}^3$ ). Therefore, the calculation result of the 45 years utilized static reserves ( $71.31 \times 10^8 \text{ m}^3$ ) is reliable.

## CONCLUSIONS

In the past 60 years, the groundwater recharge in the plain area of the Hami Basin has been continuously decreasing, and the total recharge increased from  $8.22 \times 10^8 \text{ m}^3$  in 1959 to  $4.08 \times 10^8 \text{ m}^3$  in 2020, which was mainly affected by human activities. The river valley undercurrent remained basically stable before 1996 and then decreased from  $0.35 \times 10^8 \text{ m}^3$  in 1996 to  $0.17 \times 10^8 \text{ m}^3$  in 2020. The river channel infiltration decreased slowly from  $1.65 \times 10^8 \text{ m}^3$  in 1959 to  $1.55 \times 10^8 \text{ m}^3$  in 1990, and then decreased rapidly to  $1.07 \times 10^8 \text{ m}^3$  in 2020. The leakage of canal system increased slowly from  $1.19 \times 10^8 \text{ m}^3$  in 1959 to  $1.48 \times 10^8 \text{ m}^3$  in 1990, and then decreased rapidly to  $0.5 \times$

$10^8 \text{ m}^3$  in 2020. The field infiltration remained basically stable at  $0.55 \times 10^8 \text{ m}^3$  before 1996, and then continuously decreased to  $0.18 \times 10^8 \text{ m}^3$  by 2020. The variation of groundwater conversion recharge experienced three stages: stable, rapidly decrease and slowly decrease. From 1959 to 1975, it was basically maintained at  $2.7 \times 10^8 \text{ m}^3$ , which decreased from  $2.7 \times 10^8 \text{ m}^3$  in 1975 to  $0.36 \times 10^8 \text{ m}^3$  in 2003, and then to  $0.18 \times 10^8 \text{ m}^3$  in 2020. Such reduction could be attributed to the rapid decrease of groundwater, the gradual increase of water utilization of coefficient of canal and field, and gradual decrease of groundwater level.

The groundwater discharge experienced a three-stage process of stable, slowly decrease, and rapidly decrease. The groundwater discharge was  $8.21 \times 10^8$ ,  $8.32 \times 10^8$ ,  $7.88 \times 10^8$ , and  $5.67 \times 10^8 \text{ m}^3$  in 1959, 1996, 2016, and 2020, respectively. The evapotranspiration was basically stable at  $3.39 \times 10^8 \text{ m}^3$  before 1975, and then decreased to  $1.14 \times 10^8 \text{ m}^3$  in 2020. The production of driven wells experienced three stages: slow increase, rapid increase, and decrease. It reached the peak of  $6.21 \times 10^8 \text{ m}^3$  in 2016 and then decreased to  $4.21 \times 10^8 \text{ m}^3$  in 2020. The overflow of spring water gradually decreased from  $2.14 \times 10^8$  to  $0.11 \times 10^8 \text{ m}^3/\text{a}$ . The number and discharge of karez wells decreased rapidly at first, and then decreased slowly. The number of karez wells decreased from 437 in 1959 to 85 in 2020. The corresponding discharge decreased from  $2.65 \times 10^8$  to  $0.2 \times 10^8 \text{ m}^3$ .

From 1959 to 1975, the groundwater recharge and discharge in the Hami Basin remained basically balanced, mainly influenced by hydrological and meteorological conditions. Since the balance was broken in 1975, the groundwater discharge was always greater than the groundwater recharge, displaying a negative equilibrium state. The response of groundwater level experienced three stages:

(1) from 1975 to 1990, the decline rate of local areas gradually increased;

(2) from 1990 to 2016, the decline rate of oasis plain in the entire basin rapidly increased;

(3) from 2016 to 2020, the decline rate gradually decreased; in the past 45 years, the accumulated storage variable of the Hami Basin was  $-71.3 \times 10^8 \text{ m}^3$ ; the storage variable was  $-6.3 \times 10^8 \text{ m}^3$  from 1975 to 1990,  $-56.13 \times 10^8 \text{ m}^3$  from 1990 to 2016, and  $-8.88 \times 10^8 \text{ m}^3$  from 2016 to 2020.

#### ACKNOWLEDGMENTS

We are grateful for comments and suggestions from the Editor and anonymous reviewers.

#### FUNDING

This research was funded by the Natural Science Foundation of Xinjiang (2021D01A99) and National Natural Science Foundation of China (51969029).

#### DATA AVAILABILITY

Data cannot be made publicly available; readers should contact the corresponding author for details.

#### CONFLICT OF INTEREST

The authors of this work declare that they have no conflicts of interest.

#### REFERENCES

1. Brocque, A., Kath, J. and Reardon-Smith, K., Chronic groundwater decline: a multi-decadal analysis of groundwater trends under extreme climate cycles, *J. Hydrol.*, 2018, vol. 22, no. 16, pp. 183–195.
2. Chen, Y., Zhi L., Fan, Y. et al., Progress and prospects of climate change impacts on hydrology in the arid region of northwest China, *Environ. Res.*, 2015, vol. 139, no. 5, pp. 11–19.
3. Cheng, W.J., Xi H.Y., and Z. J. T, Analysis on Infiltration Characteristics of Hyper-concentrated Flood River Channel in Xitugou Watershed of Yangguan, Dunhuang, *J. of Soil and Water Conserv.*, 2019, vol. 33, no. 6, pp. 8–26.
4. Deng Ruijie and Lei Cuilan, Comprehensive hydro-geological survey report of Hami Basin, 1959, vol. 6, no. 3, pp. 1–165.
5. Engelenburg, J. Van, Hueting, R., Rijpkema, S., Teuling A.J. et al., Impact of changes in groundwater extractions and climate change on groundwater-dependent ecosystems in a complex hydrogeological setting, *Water Resour. Manag.*, 2017, vol. 9, no. 15, pp. 456–561.
6. Feng, H.M., Zhang, G.H., Wang, D.L. and et al., Analysis on driving force for groundwater flow field evolution in Shijiazhuang Area in recent 50 years, *J. Hydraul. Eng.*, 2014, vol. 45, no. 2, pp. 180–186.
7. Gao Jianfang and Yong, X., Evaluation of groundwater resources in Hami area, 2006, vol. 13, no. 11, pp. 1–179.
8. Li Fulin, Chen Huawei, Wang Kairan et al., Comprehensive review of groundwater-dependent ecosystems, *Adv. Water Science*, 2018, vol. 29, no. 5, pp. 9–36.
9. Li Yuanyuan, Cao Jianting, Shen Fuxin et al., Changes of renewable water resources in China from 1956 to 2010, *Science China Press*, 2014, vol. 5, no. 9, pp. 11–23.
10. Qi Xiaofan, Li Wenpeng, Cui Huqun et al., Study on the conversion mechanism of surface water and groundwater in the middle reaches of the Heihe River Basin, *Hydrogeol. Engin. Geol.*, 2022, vol. 49, no. 3, pp. 155–166.
11. Qin Jianghong and Zhenmin, Z., Hami City groundwater resources development and utilization planning report, 1997, vol. 10, no. 15, pp. 1–178.
12. Qin, G. and Junshuai, L., Evolution process and trend analysis of groundwater resources in Plain area of Turpan-Hami Basin in recent 60 years, 2021, vol. 6, no. 16, pp. 1–206.
13. Song, H., Study on field irrigation infiltration recharge based on stable isotope in Xinjiang irrigated area, Master Degree Candidate, 2019, Chang An University.
14. Sheng, Zhuping, Impacts of groundwater pumping and climate variability on groundwater availability in the Rio Grande Basin, *Ecosphere*, vol. 4, no. 20, pp. 19–46.
15. Shi, J.S., Li, G.M., Liang, X. et al., Evolution mechanism and control of groundwater in the North China Plain, *Acta Geoscientica Sinica*, 2014, vol. 35, no. 5, pp. 15–23.
16. Wu, D., Yao, Zh., Jia, F. et al., Hydro-geochemical characteristics and genetic analysis of groundwater in Ha-mi basin, Xinjiang, *J. of Arid Land Resour. and Environ.*, 2020, vol. 34, no. 7, pp. 11–20.
17. Xie, N., He, H., Li Y., Groundwater survey of coal base in Eastern Xinjiang and Groundwater survey report of Hami Basin, 2011, vol. 15, no. 66, pp. 1–189.
18. Zhang, X., Wei, W., Zhou, L., et al., Analysis on spatio-temporal evolution of ecological vulnerability in arid areas of Northwest China, *Acta Ecologica Sinica*, 2021, vol. 41, no. 12, pp. 13–26.

**Publisher's Note.** Pleiades Publishing remains neutral with regard to jurisdictional claims in published maps and institutional affiliations.